KINETIC STUDIES OF THIN FILM POLYCRYSTALLINE CUBIC BORON MONOPHOSPHIDE GROWN BY CVD

E.M. Kelder, A. Goossens, P.J. van der Put, and J. Schoonman
Delft University of Technology, Laboratory for Inorganic Chemistry,
Julianalaan 136, 2628 BL Delft, The Netherlands

The CVD growth kinetics of cubic poly-BP at atmospheric pressure was studied for the BBr_3-PBr_3-H_2 system, with main emphasis on the reactant molar ratio and the temperature. For the entire temperature range studied, the reactions obey Langmuir-Hinshelwood kinetics, where the reaction rate is controlled by the reaction of both the adsorbed boron and phosphorus species. With increasing temperature a transition in surface roughness of the deposits from smooth dense layers to grains is observed. This transition correlates with a change in reaction mechanism. At low temperatures the reaction is controlled by PBr_3 with a large heat of adsorption, whereas above 900 °C the reaction is controlled by P_2, which is thermodynamically favourable, with a small heat of adsorption. In both cases the surface diffusion of adsorbed species and subsequent incorporation in the BP crystal lattice is the rate controlling mechanism.

INTRODUCTION

Cubic boron monophosphide (BP) is a III-V semiconductor with an indirect bandgap of about 2 eV (1). Cubic BP is very hard (2) and resistant to chemical corrosion (3). It dissolves under hydrothermal conditions in concentrated nitric acid and alkali hydroxide. It oxidizes in air above 800 °C under formation of BPO_4 (4). Therefore, cubic BP is an interesting compound for thin film applications.

With semiconducting electrodes immersed in an aqueous electrolyte direct conversion of solar energy to fuel or electricity is feasible. In such photoelectrochemical (PEC) cells most semiconductor electrodes are subject to severe photocorrosion under irradiation. Protection of an unstable electrode surface by BP has previously been shown to be feasible (5).
The synthesis and characterization of two crystalline boron phosphides have been reported, i.e. cubic boron monophosphide, BP (4), and a rhombohedral boron subphosphide $B_{13}P_2$ (6). Amorphous boron phosphides, B_xP, have been described as boron rich boron phosphides (7).

In our study we are interested in the kinetics of BP-depositions and the relation with semiconducting properties of cubic-BP. Here we report on the kinetics of CVD of the polycrystalline cubic-BP using BBr_3 and PBr_3 in a hydrogen atmosphere.

EXPERIMENTAL

Thermodynamic calculations on the systems B-H-Br, P-H-Br, and B-P-H-Br were performed using Solgasmix (8) adapted for PC. Thermodynamic data

have been taken from the literature. Thermodynamic data for the amorphous phase, B_xP (7) were derived from published dissociation energies of BP into B_6P and P_2-P_4 (4,9). B_xP is assumed to be a mixture of BP and B_6P without any interaction terms.

A thermobalance CVD set-up equipped with a vertical hot wall fused silica tube reactor (ID 2 cm) as described previously (7) is used to determine growth rates of cubic poly-BP as a function of temperature and BBr_3 and PBr_3 reactant gas concentrations at atmospheric H_2 pressure. The average of the total gas flux was about 400 ml/min/cm^2.

The solid reaction products were characterized by means of Debye-Scherrer diffraction patterns. These results are discussed in (7) and summarized in Figure 1.

RESULTS

Thermodynamic calculations

The calculations for the P or B-H-Br system show which gas species could be present in the gas phase during deposition. BBr_3 almost completely transforms into solid boron and gaseous HBr with a small amount of $BHBr_2$. If we assume a homogeneous gas equilibrium without deposition of solid boron, the gas phase contains $BHBr_2$, HBr, H_2, and small amounts of other boron containing species (Fig. 2). Calculations for PBr_3 show that it is completely converted to P_2, P_4, and HBr (Fig. 3). In Figure 4 we have summarized the calculations for mixtures of PBr_3 and BBr_3 in H_2 for the solid phases. This shows that the concentration of BBr_3 must be equal to or smaller than that of PBr_3 to prevent deposition of B_xP. Experimentally, we found that even lower B/P ratios are required (Fig. 1).

Kinetic measurements

We measured the growth rate as a function of input reactant concentration and temperature. The growth rate increases almost linearly with BBr_3 concentration but drops at a higher input. A logarithmic plot of the concentration of BBr_3 versus the growth rate (Fig. 5) shows a slope of 1 for low input concentrations in the entire temperature range. At higher input concentrations the slope decreases. Such concentration dependencies are also reported for borane in the B_2H_6 - PH_3 system (10). The PBr_3 reactant shows a different pattern (Fig. 6). At zero concentration pure boron is deposited so even at this concentration a nonzero growth rate is observed. At very low PBr_3 concentration where $PBr_3/BBr_3 < 1$ and B_xP is formed (7), we observe a slight increase in the growth rate due to phosphorus incorporation in the boron matrix. At a certain concentration a steep increase in the growth rate is observed due to the formation of cubic BP (7). At increasing PBr_3 concentration the growth rate shows a maximum and decreases exponentially. The logarithmic plot (Fig. 7) shows a slope of -1 between 800 and 900 °C at high PBr_3 concentrations. This order in PBr_3 changes to -1/2 between 930 and 1030 °C. The decrease in the growth rate, by increasing PBr_3 concentration, has also been reported for PCl_3 (2,11). Activation energies can be derived from these measurements assuming certain reaction mechanism models.

DISCUSSION AND CONCLUSIONS

In table 1, gas phase reactions involving the main gaseous species [1-3], adsorption equilibria of these species [4-10], and possible surface reactions which yield BP [11-15] are listed. An expression for the deposition rate is given [4a-15a] if the corresponding reaction would be rate limiting. BBr_3 is assumed to react directly to $BHBr_2$ [1] in the gas phase which in its turn is assumed to be the reactive boron gas species. From the lack of a square-root dependence on the BBr_3 concentration we conclude that HBr does not adsorb after dissociation of $BHBr_2$, according to equation 5, into BBr and HBr. The observed decrease in the growth rate with the PBr_3 gas concentration indicates that surface adsorption effects determine the reaction mechanism. The maxima found indicate that the corresponding adsorbed species compete for the same adsorption sites (7), and therefore, the kinetics obey Langmuir-Hinshelwood behaviour (12).

The rate equations involving only adsorption of a boron species [4], dissociation on the surface of a boron species [5], or a reaction of an adsorbed boron species with the gas phase [6,11-13] are not consistent with the observed rate dependence of PBr_3. The equations involving only adsorption of a phosphorus species [7-9], or reaction of an adsorbed phosphorus species with the gas phase [10], would imply positive slopes, decreasing to zero at very high PBr_3 concentration instead of the decreasing rate found experimentally. Hence both adsorbed reactant species determine the overall deposition rate, which means that only reaction [15] can be rate limiting. The rate equation 15a explains the observed effects of the concentration of both reactants, irrespective of the identity of the adsorbing species. A reaction order of -1 in PBr_3 is possible if PBr_3 adsorbs competitively with a boron species. Then the complete reaction rate is (7):

$$R = \frac{k_r * K_B * K_P * p_B * p_P}{(1 + K_B * p_B + K_p * p_P)^2} \qquad 17$$

The following constants result from a least squares fit:

$k_r = \exp\{ -25470/T + 23.07 \}$ $\quad \Delta H_r = -212$ kJ/mole
$K_B = \exp\{ 25540/T - 28.19 \}$ $\quad \Delta H_B = 212$ kJ/mole
$K_P = \exp\{ 8250/T - 11.18 \}$ $\quad \Delta H_P = 68.6$ kJ/mole

k_r, ΔH_r : reaction rate constant, reaction activation energy
K_B, ΔH_B : adsorption constant, heat of adsorption for the B-species
K_P, ΔH_P : adsorption constant, heat of adsorption for the P-species

The presence of undissociated PBr_3 is corroborated by the detection of PBr_3 in the outlet of the reactor at these temperatures. At higher deposition temperatures, no PBr_3 leaves the reactor. Above 900 °C the reaction order in the PBr_3 reactant is -1/2, which could be caused by dissociative adsorption of P_2 which is in this temperature range thermodynamically in excess compared to P_4. For this temperature range the complete equation for the reaction rate is:

$$R = \frac{k_r * K_B * K_P^{0.5} * p_B * p_P^{0.5}}{(1 + K_B * p_B + K_P^{0.5} * p_P^{0.5})^2} \qquad 18$$

The following constants result from a least squares fit:

$k_r = \exp\{ -28710/T + 26.02 \}$ $\quad \Delta H_r = -248$ kJ/mole
$K_B = \exp\{ 25540/T - 28.19 \}$ $\quad \Delta H_B = 212$ kJ/mole
$K_P = \exp\{ 3220/T - 6.60 \}$ $\quad \Delta H_P = 26.8$ kJ/mole

The heat of adsorption for the boron species is taken to be the same as in equation 17. The activation energies for both temperature regimes are the same since the same reaction [15] is rate limiting. The activation energy is controlled by surface diffusion or by incorporation of BP in the crystal lattice. At low temperatures, although P_4 is abundant, the formation of BP is dictated by PBr_3, whereas at high temperature where PBr_3 is completely dissociated, the formation is dictated by P_2. At even higher temperatures a diffusion controlled regime occurs. Then the diffusion of the boron reactant is limiting, since B_xP is expected to be formed if the supply of boron is abundant.

As reported earlier (7), a transition is found in the surface morphology of the deposits from smooth dense films to grains. If we compare the surface of the deposits on fused silica and sintered polycrystalline alumina substrates, it is observed that nucleation sites play an important role in the growth of BP. On fused silica where nucleation is difficult because of lack of suitable sites, amorphous B_xP is found (Fig. 1), which suggests that the phosphorus species is poorly adsorbed on clean surfaces. This is corroborated by the low heat of adsorption compared to the heat of adsorption of PBr_3. This means that for the formation of smooth dense cubic BP films at high temperatures the phosphorus input reactant should be sufficiently stable in a thermodynamic or kinetic sense to prevent grain growth on the surface. This is already observed for the PCl_3 reactant (2) which is thermodynamically more stable than PBr_3. Lindstrom et al. (2) have shown pictures where the transition can be observed in the surface morphology between 1050 and 1100 °C, although they did not mention this. It is also confirmed by Nishinaga et al (11), who did not observe any regular pattern in the growth morphology beyond 1070 °C. The films grown at 1080 °C were polycrystalline and were broken into fine pieces when the substrate silicon was removed by chemical etching (11). Chu et al (13) who used the very unstable hydride reactants observe nucleation in the gas phase at temperatures in excess of 900 °C.

A better method to prevent excessive P_2 formation is the use of a cold wall reactor, where gas phase reactions occur only in the thin diffusion layer near the surface. The decomposition rate of PBr_3 is probably reduced compared to a hot wall reactor. In our laboratory, we have in fact grown epitaxial layers of cubic BP on silicon in the temperature range between 900 and 1000 °C (14), in a cold wall reactor.

The surface concentrations, calculated for several temperatures for PBr_3 input in the regime for BP growth (Table 2), in both regimes, show that although there is a change in reaction mechanism the surface

concentration of the phosphorus is still in excess. This excess of phosphorus, needed to prevent growth of amorphous B_xP, is likely to be incorporated into the lattice of cubic BP, which therefore becomes an n-type semiconductor (14). The fact that we always obtain n-type cubic BP without any annealing technique supports this model.

REFERENCES

1. C. C. Wang, M. Cardona and A. G. Fischer, RCA Rev., 25, 159, (1964)
2. J. Lindstrom, K. Fundell and A. Lind, Proc. 4th Intern. Conf. on CVD, 547, (1973)
3. T. Mizutani, H. Asano, T. Nishiniga and S. Uchiyama, Jap. J. Appl. Phys., 16, 1629, (1977)
4. F. V. Williams and R. A. Ruehrwein, J. Amer. Chem. Soc., 82, 1330, (1960)
5. R. J. Baughman and D. S. Ginley, J. Solid State Chem., 50, 189, (1983)
6. R. A. Burmeister and P. E. Greene, Bull. Am. Phys. Soc., 10, 1184, (1965)
7. E. M. Kelder, A. Goossens, P. J. van der Put and J. Schoonman, Proc. EuroCVD seven, C5-667, (1989)
8. G. Eriksson, Chemica Scripta, 8, 100, (1975)
9. A. S. Alikhanyan, A. V. Steplevskii, Ya. Kh. Grimberg and V. I. Gorgoraki, Russ. J. Phys. Chem., 49 (12), 1846, (1975)
10. K. Shohno, H. Ohtake and J. Bloem, J. Cryst Growth, 45, 187, (1978)
11. T. Nishinaga and T. Mizutani, Jap, J. Appl. Phys., 14, 753, (1975)
12. M. E. Jones and D. W. Shaw, in "Treatise on solid state chemistry, Vol 5", Ch 6, (1974)
13. T. L. Chu, J. M. Jackson, A. E. Huslop and S. C. Chu, J. Appl. Phys., 42, 420, (1981)
14. A. Goossens, E. M. Kelder and J. Schoonman, Ber. Bunsenges. Phys. Chem., 93, 1109, (1989)

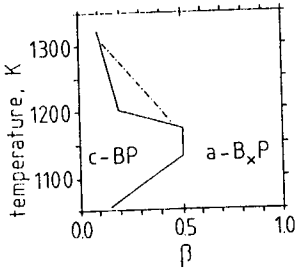

Fig. 1. CVD diagram of the observed solid phases in the system BBr_3-PBr_3 at atmospheric H_2 pressure.
----- : fused silica substrate;
-.-.- : sintered alumina substrate
β = $p(BBr_3)$ / ($p(BBr_3)$ + $p(PBr_3)$).

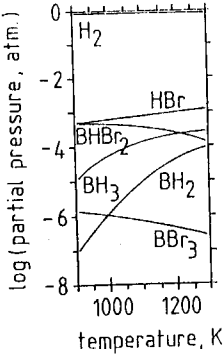

Fig. 2. Calculated gas phase composition in the B-H-Br system as function of temperature at atmospheric H_2 pressure, $p(BBr_3)$=50 Pa.

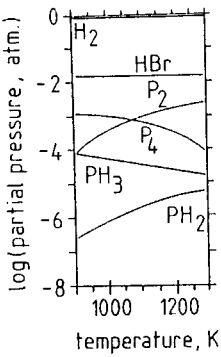

Fig. 3. Calculated gas phase composition in the P-H-Br system as function of temperature at atmospheric H_2 pressure, $p(PBr_3)$ = 500 Pa.

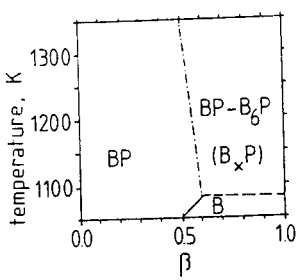

Fig. 4. Calculated solid phase diagram in the system BBr_3-PBr_3 at atmospheric H_2 pressure, for reactant concentrations between 0.1 and 1 %.

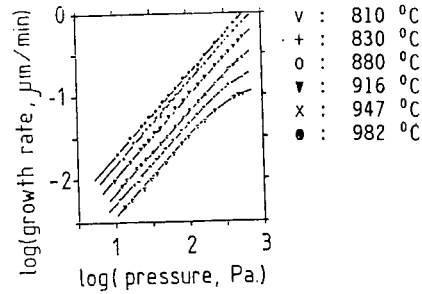

Fig. 5.Logarithmic plot of the growth rate versus BBr_3 pressure for several temperatures; $p(PBr_3)$= 485 Pa.

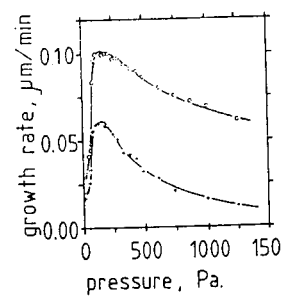

Fig. 6. Growth rate versus PBr_3 pressure at 840 °C (+), and 1008 °C (o), $p(BBr_3)$= 45 Pa.

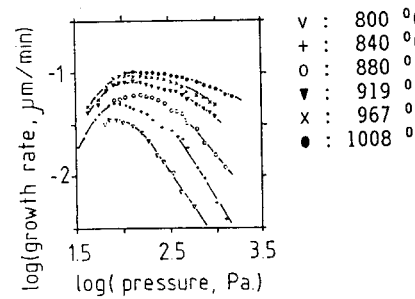

Fig. 7.Logarithmic plot of the growth rate versus PBr_3 pressure for several temperatures; $p(PBr_3)$= 45 Pa.

Table 1. Reaction mechanism model with calculated growth rates.

REACTION		GROWTH RATE	
$BBr_3 + H_2 \rightleftharpoons BHBr_2 + HBr$	1		
$4\ PBr_3 + 6\ H_2 \rightleftharpoons P_4 + 12\ HBr$	2		
$P_4 \rightleftharpoons 2\ P_2$	3		
$BHBr_2 + s \rightleftharpoons BHBr_2.s$	4	$k_{r_4}^* p_{BHBr_2}^* \theta_s$	4a
$BHBr_2.s \rightleftharpoons BBr.s + HBr$	5	$k_{r_5}^* \theta_{BHBr_2}$	5a
$BBr.s + 0.5\ H_2 \rightleftharpoons B.s + HBr$	6	$k_{r_6}^* p_{H_2}^{0.5} * \theta_{BBr}$	6a
$0.5\ P_2 + s \rightleftharpoons P.s$	7	$k_{r_7}^* p_{P_2}^{0.5} * \theta_s$	7a
$0.25\ P_4 + s \rightleftharpoons P.s$	8	$k_{r_8}^* p_{P_4}^{0.25} * \theta_s$	8a
$PBr_3 + s \rightleftharpoons PBr_3.s$	9	$k_{r_9}^* p_{PBr_3}^* \theta_s$	9a
$PBr_3.s + 1.5\ H_2 \rightleftharpoons P.s + 3\ HBr$	10	$k_{r_{10}}^* p_{H_2}^{1.5} * \theta_{PBr_3}$	10a
$B.s + 0.5\ P_2 \rightleftharpoons <BP> + s$	11	$k_{r_{11}}^* p_{P_2}^{0.5} * \theta_B$	11a
$B.s + 0.25\ P_4 \rightleftharpoons <BP> + s$	12	$k_{r_{12}}^* p_{P_4}^{0.25} * \theta_B$	12a
$B.s + PBr_3 + 1.5\ H_2 \rightleftharpoons <BP> + 3\ HBr + s$	13	$k_{r_{13}}^* p_{PBr_3}^* p_{H_2}^{1.5} * \theta_B$	13a
$P.s + BHBr_2 + 0.5\ H_2 \rightleftharpoons <BP> + 2\ HBr + s$	14	$k_{r_{14}}^* p_{H_2}^{0.5} * p_{BHBr_2}^* \theta_P$	14a
$P.s + B.s \rightleftharpoons <BP> + 2\ s$	15	$k_{r_{15}}^* \theta_B^* \theta_P$	15a

Table 2. Surface concentration at several temperatures.

T, °C	θ_P	θ_B	eq.
800	0.63	0.13	17
850	0.64	0.064	17
950	0.56	0.013	18
1000	0.55	0.006	18

s = adsorption site
θ_i = fractional surface concentration of specie i

$$\theta_i = (K_i^{\alpha} * p_i^{\alpha})/(1+K_i^{\alpha} * p_i^{\alpha} + \Sigma K_j^{\beta} * p_j^{\beta}) \quad 16$$

$\Sigma K_j^{\beta} * p_j^{\beta}$ = sum of all other species

α = dissociation order of specie i
β = dissociation order of specie j
K_i = adsorption constant of specie i
K_j = adsorption constant of specie j
k^{r_1} = reaction rate constants
p_i = gas phase concentration of specie i